Superconducting Power Filter for Aircraft Electric DC Grids

Frederic Trillaud, Bruno Douine, Loic Queval

DOI: http://doi.org/10.1109/TASC.2021.3060682 & URL: https://ieeexplore.ieee.org/document/9359489. Cite: F. Trillaud, B. Douine, L. Quéval*, "Superconducting power filter for aircraft electric DC grids" IEEE Transactions on Applied Superconductivity, vol. 31, no. 5, pp. 1-5, Aug. 2021.

Superconducting power filter for aircraft electric DC grids

Frederic Trillaud, Bruno Douine, Loïc Quéval

***Abstract*—A new device, referred to as Superconducting Power Filter (ScPF), is introduced to improve the stability of aircraft electric DC grids. This device is made of a non-inductive superconducting coil connected in series with a conventional RLC filter. The superconducting coil behaves as a nonlinear current-dependent resistance. By design, the superconductor does not undergo a full transition to the normal-resistive state and remains in the current-sharing regime. Thus, a quick response and recovery of the superconductor to transients can be achieved. In the present work, the thermo-electric model of the device incorporates a refined description of the transition from the superconducting state to the normal-resistive state of the superconductor. To check the feasibility of passive stabilization of embedded DC grids using ScPF, different widths and lengths of commercially available 2nd generation High Temperature Superconducting (2G HTS) tapes were considered. We chose a case study simulating an equivalent circuit of a More Electric Aircraft (MEA) with an EPS-A3 architecture. For this particular case study, it is shown that the stability limit of the DC grid can be significantly increased, while preserving the reliability (no quench) and low cost (only a few meters of superconducting tape) of the ScPF.**

***Index Terms*—More Electric Aircraft, embedded DC grid, stability, superconducting power filter, thermo-electric model.**

I. Introduction

SOME architectures of modern electric aircraft may be relying on DC grids [1], [2]. As all DC grids, stability can be an issue when the power demand varies abruptly due to the interaction between the source and the load [3]. The simplest therefore robust approach to deal with stability of DC links is a conventional RLC passive filter. The short-coming of such approach is the limited range of stability offered by predetermined values of resistance, inductance and capacitance. More complex technologies rely on active measures to get a dynamic response [4]. However, the drawbacks of implementing additional systems are the decrease in reliability and in efficiency which are two important parameters in aircraft applications. Therefore, an alternative passive technology, referred to as Superconducting Power Filter (ScPF) or superconducting stabilizer is proposed here. It combines a resistive superconducting component (SCC) with a classic RLC filter [5]. In its construction, the SCC is similar to a resistive Fault-Current Limiter (r-ScFCL) [6]. However, it is operated in the current-sharing regime of the superconductor to behave as a dynamic resistance. Thus, it provides stability with operational safety margin since the superconductor never undergoes a full transition from the superconducting state to the normal-resistive state by design [7].

Hereinafter, a refined model of the ScPF is presented. This model is an improvement on previous thermo-electric models published for r-ScFCL [8], [9] by adding an additional level of details of the transition from the superconducting to the normal-resistive state of the superconductor, namely the current-sharing regime of 2G HTS tapes [10].

In the present work, the equivalent DC grid of an electric aircraft is simulated and the impact of the design of the ScPF on its stability is analyzed. For different widths of commercial REBCO tapes therefore different values of critical current, the minimum lengths required to ensure stability under the requirement that the SCC should be operated in current-sharing regime are estimated. Using the RLC filter as reference, it is shown that the power stability limit can be significantly extended at short lengths of HTS tape (a few meters). This makes the ScPF an attractive solution to push further the stability of existing DC links for modern aircraft electric DC grids.

II. Design of the ScPF

The ScPF is constituted of a SCC connected in series with a conventional RLC filter. The latter provides a baseline to the power stability limit. The SCC follows the same design as a r-ScFCL and adds a dynamic resistance to the overall filter. Thus, the winding of the superconducting coil is such that its inductive component is canceled [11]. An additional metallic shunt resistor, located at room temperature, is connected in parallel to the superconducting coil to add an additional control on the amount of resistance reached by the device during a transient event as well as enabling a passive protection to the superconducting coil to avoid any damages to the SCC in case of extreme events. As a result, the SCC resistance depends solely on the current, going from zero when the current is well below the critical current of the SCC $I_{c,scc}$ to a dynamically changing value around and above $I_{c,scc}$. In the following study, the SCC is wound with a single non-insulated commercial Cu-stabilized 2G HTS tape with a 20 μm layer of Cu on both side of the tape, 2 μm layer of Ag, a 1 μm layer of REBCO, a negligible 0.2 μm of buffer layers (not considered in the model), a 50 μm layer of Hastelloy, a 1.8 μm

This work was funded in part by the Dirección General de Asuntos del Personal Académico (DGAPA) of the Universidad Nacional Autonóma de Mexico (UNAM) under grant DGAPA-PAPIIT 2019 (#IN107119), and in part by the GDR SEEDS under grant AAP 2019 ScPF. (*corresponding authors: L. Quéval and F. Trillaud*)

F. Trillaud is with the Instituto de Ingeniería, Universidad Nacional Autonóma de Mexico, 04510 Ciudad de Mexico, Mexico (e-mail: ftrillaudp@ii.unam.mx).

L. Quéval is with the Group of Electrical Engineering - Paris (GeePs), University of Paris-Saclay, CentraleSupélec, CNRS, 91192, Gif-sur-Yvette, France and with Sorbonne University, CNRS, 75252, Paris, France. (e-mail: loic.queval@geeps.centralesupelec.fr).

B. Douine is with the Groupe de Recherche en Energie Electrique de Nancy, University of Lorraine, Vandoeuvre-lès-Nancy 54 506, France (e-mail: bruno.douine@univ-lorraine.fr).

layer of Ag as manufactured by Superpower Inc.. Its shunt resistor has a resistance R_{sh} equal to 10 mΩ. In the present work, different tape widths and lengths are compared. From the manufacturer's catalogue, for a Cu stabilized tape [12], the widths and the corresponding minimum critical currents measured at 77 K in self-field (I_{c0}) are: 2 mm (50 A), 3 mm (75 A), 4 mm (100 A), 6 mm (150 A) and 12 mm (300 A).

III. Improved Thermo-Electric Model

Some key aspects of the model and equations are recalled hereinafter. Additional information can be found in [9], [13]. The main assumptions are: (1) the tape has homogeneous and isotropic properties along its length, (2) its entire length undergoes the same transition during transients, (3) it is evenly and fully cooled by LN2 at T_{LN2} = 77 K [14], (4) its critical current is the critical current of the SCC. Under these assumptions, the heat balance equation is solved across the thickness of the different layers of the tape using an implicit scheme as follows,

$$\mathbf{T}_{t+\Delta t} \simeq \left(\mathbb{C}_{p,t} - \Delta t \mathbb{W}_t\right)^{-1} \left[\Delta t \left(\mathbf{P}_t - \mathbf{Q}_t\right) + \mathbb{C}_{p,t} \mathbf{T}_t\right] \quad (1)$$

where t represents the current time and Δt the time step. $\mathbf{T}$ gathers the temperature computed at the center of each layer. Since the shunt resistor is located at room temperature, it is not included in the thermal model. The different tape layers dissipate active power according to $\mathbf{P} = \mathbb{R}\ \mathbf{i}.\hat{}2$ (element-wise square power), with $\mathbb{R}$ a matrix lumping the resistances of the tape layers and $\mathbf{i}$ a vector of the currents flowing in the corresponding layers during current redistribution. The surfaces of upper and lower Cu stabilizers exchange heat power $\mathbf{Q}$ with the LN2. The corresponding heat flux depends on the temperature difference between the bare Cu surface and the liquid nitrogen. The matrix of resistance $\mathbb{R}$, the matrix of heat capacity $\mathbb{C}_p$ and the matrix of thermal conductances $\mathbb{W}$ depend on temperature through the resistivity, specific heat capacity and thermal conductivity of the different materials making the tape layers. The temperature dependence of the material properties were found in the database of the National Institute of Standards and Technology (NIST) [15].

The voltage drop along the tape v_{scc} is given by [16] as,

$$v_{scc} = V_c \left(\frac{i_{sc}}{I_c}\right)^n \quad (2)$$

where $V_c = l_{tp} E_c$ is the critical voltage across the length of the tape l_{tp} ($E_c = 1\ \mu$V/cm), i_{sc} is the current flowing through the superconducting layer and n is the transition index which depends on temperature as presented in [9]. The critical current I_c of the tape depends linearly on the temperature of the superconductor as in [17], and,

$$\begin{cases} I_c = I_{c0}, & T_{LN2} \le T \le T_{cs} \\ I_c = I_{c0} \left(\dfrac{T_{cs} - T}{T_{cs} - T_c}\right), & T_{cs} < T \le T_c \\ I_c = 0, & T > T_c \end{cases} \quad (3)$$

where I_{c0} is the minimum critical current measured at T_{LN2} in self-field and T_c is the critical temperature of the superconductor equal to 92 K. The current sharing temperature T_{cs} is given by,

$$T_{cs} \simeq T_c + (T_{LN2} - T_c) \frac{|i|}{I_{c0}} \quad (4)$$

To obtain the current distribution in the different tape layers and the shunt resistor, it is necessary to solve,

$$\begin{cases} V_c \left(\frac{i_{sc}}{I_c}\right)^n + R_{m,sh} \left(i_{sc} - i\right) = 0, \\ i = i_{sc} + i_m + i_{sh} \end{cases} \quad (5)$$

where i_{sh} and i_m are the fractions of total current i flowing in the shunt resistor and the metallic layers of the tapes, respectively. $R_{m,sh}$ is the equivalent resistance of the combined metallic layers and shunt. The current in each layer k including the shunt is derived as $i_k = (R_{SCC}/R_k)\, i$, with R_{SCC} the equivalent resistance of the SCC and R_k the resistance of the layer k.

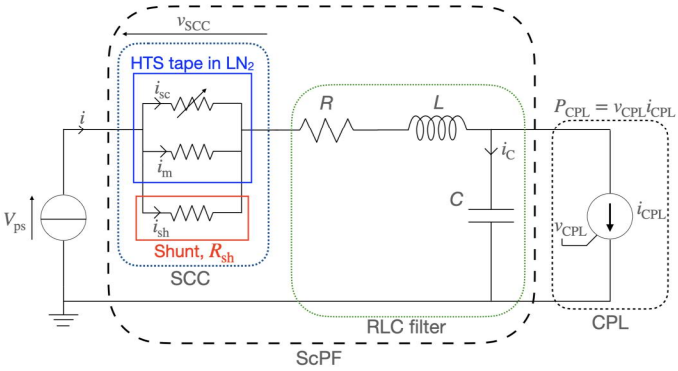

Fig. 1: Case study: equivalent DC grid. The power source (PS) supplies the controlled power load (CPL) through a ScPF.

IV. Aircraft DC Grid with ScPF

Figure 1 illustrates the equivalent DC grid for a possible More Electric Aircraft (MEA). The model is generic whereas the values of the electric circuit are provided by the choice of the specific architecture of type EPS-A3 such as found in the Boeing 787 [18]. The source is modeled by an ideal voltage source V_{ps} which supplies a constant power load (CPL) through the ScPF. The parameters of the DC electrical circuit are: $V_{ps} = 540$ V, $R = 10$ mΩ, $L = 10\ \mu$H, and $C = 500\ \mu$F. The corresponding simulation was carried out with Simulink Simscape Electrical toolbox.

For aircraft application, we propose the following stability criteria to design the ScPF for a stable operation of the DC link:

1) the maximum temperature reached by the SC layer $T_{sc,max}$ during the power surge should be less than 90 K so that the superconductor exclusively operates in its current-sharing regime
2) the load voltage should be strictly positive at all time: $v_{CPL} > 0$
3) the peak-to-peak load voltage oscillations at the load must be less than 1‰ of the average load voltage before the end of the power surge,

$$\exists t^\star \in (t_i + \tau + \tau_p, t_i + \tau + \Delta t_p) \Rightarrow$$
$$\Delta v_{CPL}(t^\star) \le 0.001 \times \underbrace{\left(\frac{1}{\tau_p} \int_{t^\star - \tau_p}^{t^\star} v_{CPL}\, dt\right)}_{\bar{v}_{CPL}} \quad (6)$$

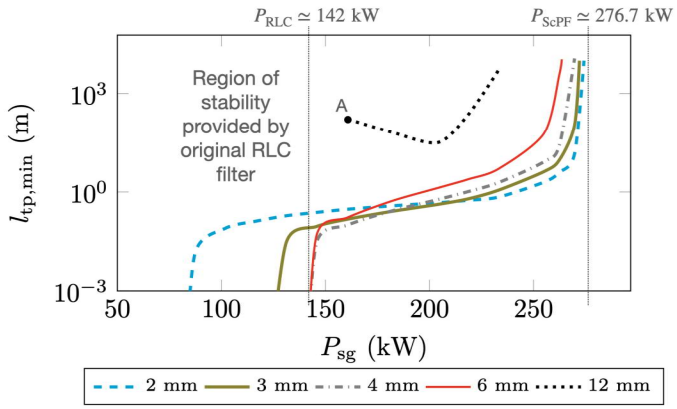

Fig. 2: Minimum tape length $l_{\mathrm{tp,min}}$ versus magnitude of the power surge P_{sg}. The point "A" (160.8 kW or 113%$P_{\mathrm{RLC,an}}$) indicates the lowest limit on stability for the 12 mm wide tape.

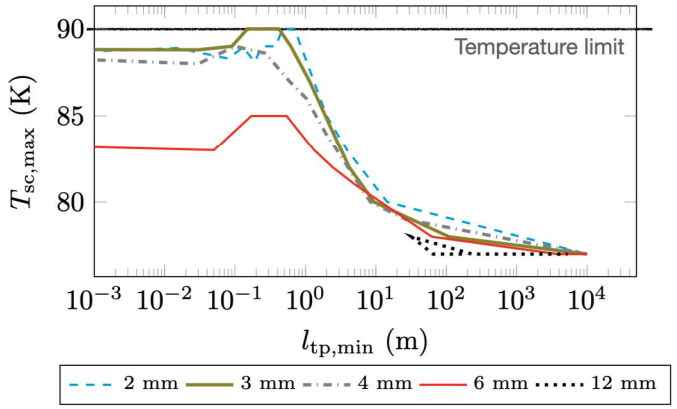

Fig. 3: Maximum temperature of the superconductor layer $T_{\mathrm{sc,max}}$ as a function of the minimum tape length $l_{\mathrm{tp,min}}$.

with τ_{p} the period of the voltage oscillations, τ the rise and fall time of the power surge and Δt_{p} the duration of a power surge.

V. Results of Simulations

For the different tape widths, the minimum length of conductor necessary to ensure stability during transients power surges are assessed. The power surges start at $t_{\mathrm{i}} = 0.1$ s and last for $\Delta t_{\mathrm{p}} = 0.7$ s with a rise and fall time τ equal to 0.1 s at a peak power P_{sg}.

A. Minimum tape length

Without the ScPF, the simulated power stability limit P_{RLC} was found equal to 142 kW under the proposed design criteria[1]. Figure 2 shows the evolution of the minimum tape length $l_{\mathrm{tp,min}}$ as a function of the peak power P_{sg}. As the power is increased, the minimum tape length initially increases at a slow rate. Then, when the power approaches a new power limit, referred to as P_{ScPF}, equal to 195%P_{RLC} (276.7 kW), the minimum tape length diverges (meaning that no design can satisfy the stability criteria). It is recalled that, due to the chosen criteria for the SCC design, the full transition to the normal-resistive state of the superconductor (SC) layer is not permitted, therefore, the power stability limit with the ScPF is asymptotically achieved being strictly less than the power limit given by the maximum resistance of the ScPF obtained at full transition of the SC layer, i.e. $R + R_{\mathrm{sh}}$, as discussed in [7].

[1]The classic analytical limit of power stability provided by the RLC filter is recalled here for completeness, $(RC/L)V_{\mathrm{ps}}^2 = 145.8$ kW.

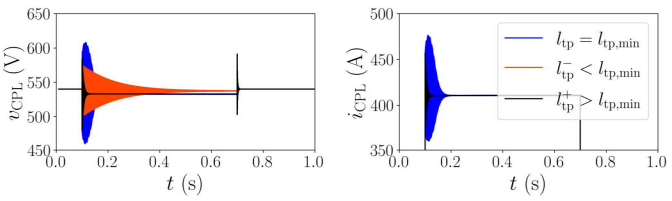

Fig. 4: Load voltage (left) and load current (right) for P_{sg}=154%$P_{\mathrm{RLC,an}}$ (218.7 kW) and a tape width of 3 mm for different tape lengths.

At powers below 180%P_{RLC} (255.15 kW), the tape length is of the order of meters for tape widths between 2 mm and 6 mm. For the 12 mm wide tape, the minimum tape length is of the order of tens of meters. For this particular tape width, it was found that it is not possible to damp the voltage oscillations below 113%P_{RLC} (160.8 kW, point "A" in Fig. 2) at any tape lengths. Indeed, the current drawn by the load is well below the critical current and the temperature of the superconductor, as shown in Fig. 3, remains close to the initial operating temperature resulting in an insufficient value of SCC resistance (of the order of tenths of milliOhm) to damp the load voltage oscillations.

There is an overall tendency for the power stability limit to diminish and $l_{\mathrm{tp,min}}$ to increase as the tape width is increased (Fig. 2). A combined effect arises between the increase in the capacity of extracting heat through a larger tape width (larger exchange surface with LN2) and the decrease in dissipation at greater critical currents that lessens the SCC resistance which limits the increase in temperature of the SC layer (of the order of milliKelvin). As shown in Fig. 3, more tape length is then necessary to achieve the resistance required to address the load voltage oscillations. By adding more length, the resistance of the superconductor still builds up following the power law as the current gets closer or greater than the SCC critical current (2).

The maximum power stability limit is achieved with a tape width of 2 mm with a 80% increase of the power stability limit on top of the power stability limit of the RLC filter. However, the minimum tape length required is of the order of thousands of meters (see Fig. 2). Furthermore, as in the case of the 3 mm wide tape, the minimum tape length is non-zero below P_{RLC} which indicates that the ScPF will operate and therefore dissipates energy under the stability limit of the RLC filter alone. It is not desired as the main idea is to minimize the losses below the stability limit of the RLC filter and provides extra stability margin above. Thus, the best trade-off is given by the 6 mm wide tape with a power gain of 54% on top of the power stability limit of the RLC filter at a maximum temperature of 82 K well below the temperature criterion and a tape length of only 2.44 m without power dissipation under the power stability limit of the RLC filter as shown in Fig. 2 (zero $l_{\mathrm{tp,min}}$ at P_{RLC}).

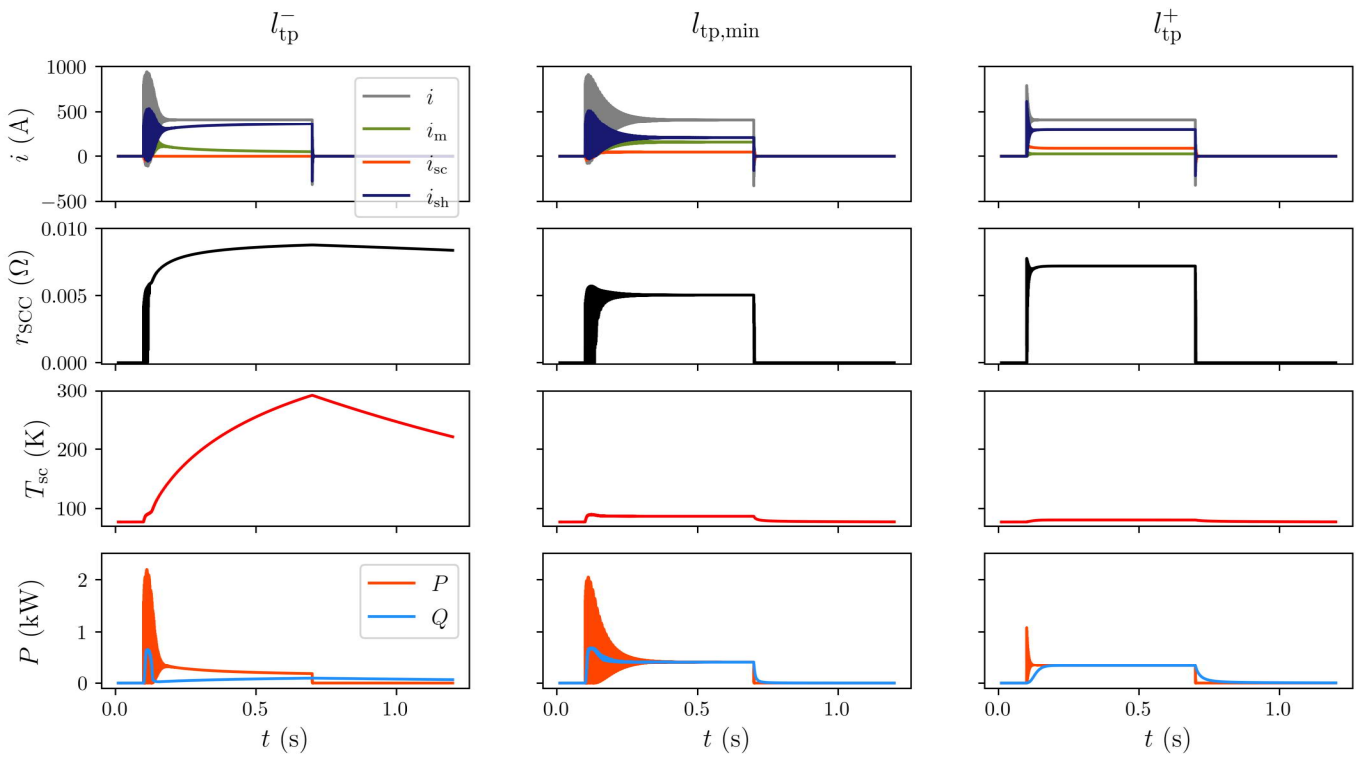

Fig. 5: Thermo-electric behavior of the SCC for 154%$P_{RLC,an}$ (218.7 kW) and a tape width of 3 mm. Left figures: l_{tp}^{-} = 0.57 m, center figures: $l_{tp,min}$ = 0.6 m, and right figures: l_{tp}^{+} = 6 m.

B. Response of the SCC around the minimum tape length

Figure 4 shows the voltage and the current of the load for a power surge equal to 154%P_{RLC} (218.7 kW), a tape width equal to 3 mm and three cases of tape length: 1) at the minimum tape length ($l_{tp,min}$ = 0.6 m), 2) at a shorter tape length (l_{tp}^{-} = 0.57 m), and 3) at a larger tape length (l_{tp}^{+} = 6 m). Fig. 5 shows the corresponding results of the thermo-electric behavior of the SC layer and the SCC for the three cases. At the shorter tape length l_{tp}^{-}, the SC layer undergoes a full transition from the superconducting state to the normal-resistive state ($T_{sc} > T_c$). At the minimum tape length $l_{tp,min}$ and at a larger tape length l_{tp}^{+}, the SC layer remains in the current-sharing regime ($T_{sc,max} < 90$ K). For all the three cases, the current redistributes mainly between the metallic layers of the tape and the shunt resistor which provides the necessary damping to stabilize quickly the current and voltage as shown in Fig 4. At $l_{tp,min}$, enough dissipation is generated to drive the temperature T_{sc} above the current-sharing temperature T_{cs} which provides enough resistance to reduce the load voltage oscillation below 1‰ of the average load voltage. As the tape length is increased beyond the minimum tape length, $l_{tp}^{+} > l_{tp,min}$, the maximum temperature of the SC layer decreases accordingly to reach a value lower than the current-sharing temperature T_{cs}. However, as discussed in the subsection V-A, despite a temperature close to the initial operating temperature, the current flowing through the SCC is significantly larger than the critical current and the current mainly redistributes into the shunt resistor thereby dominating the resistance value of the SCC. By increasing the tape length, it is possible to push further the power stability limit while operating the SCC even below the current-sharing regime facilitating the compliance with the design criteria of the ScPF. At l_{tp}^{-}, no thermal equilibrium can be achieved as the superconductor quenches over the duration of the power surge reaching a maximum temperature of 272 K. However, such an extreme operation is prohibited by design.

For all three cases, the dissipated power P remains of the order of kiloWatts which can be taken out by a cryo-refrigerator based on liquid nitrogen at 77 K as part of the aircraft design [19], [20], [21].

VI. Conclusion

The issue of stability of a DC grid in a More Electric Aircraft can be effectively addressed by a compact LN2-cooled 2G HTS Power Filter. The results obtained on an equivalent circuit model of an existing EPS-A3 type architecture showed that the stability limit can be significantly increased. Depending on the tape critical current arising from the choice of tape width, the ScPF can be operated in the current-sharing regime of the superconductor thereby increasing its reliability. For its design, a trade-off between the maximum temperature of the SC layer (safety margin) and the tape length (cost) has to be considered for a safe and reliable operation of the ScPF during transients. The same device could be implemented in an hydrogen-powered aircraft. Indeed, the liquid hydrogen (LH2) could then be used as indirect coolant for the LN2-cooled HTS stabilizer. For better integration, future work may look at a fully LH2-cooled device using MgB_2 wires for the SCC. Further considerations can include the design of the associated cryogenic system to assess the weight of the system to be compared to alternative technological solutions.

REFERENCES

[1] J. Brombach, A. Lücken, B. Nya, M. Johannsen, and D. Schulz, "Comparison of different electrical HVDC-architectures for aircraft application," in *2012 Electrical Systems for Aircraft, Railway and Ship Propulsion*, 2012, pp. 1–6.

[2] Xin Zhao, J. M. Guerrero, and Xiaohua Wu, "Review of aircraft electric power systems and architectures," in *2014 IEEE International Energy Conference (ENERGYCON)*, 2014, pp. 949–953.

[3] K. N. Areerak, T. Wu, S. Bozhko, G. M. Asher, "Aircraft Power System Stability Study Including Effect of Voltage Control and Actuators Dynamic," *IEEE Transactions on Aerospace and Electronic Systems*, vol. 47, no. 4, pp. 2574–2589, 2011.

[4] D. Riua, M. Sautreuila, N. Retiére, O. Sename, "Control and design of DC grids for robust integration of electrical devices. Application to aircraft power systems," *International Journal of Electrical Power & Energy Systems*, vol. 58, pp. 181–189, 2014.

[5] G. Huang, B. Douine, K. Berger, , G. Didier, I. Schwenker, J. Lévêque, "Increase of Stability Margin in Embedded DC Electric Grid With Superconducting Stabilizer," *IEEE Transactions on Applied Superconductivity*, vol. 26, no. 4, p. 5000304, 2016.

[6] J. Bock, A. Hobl, J. Schramm, S. Krämer, C. Jänke, "Resistive Superconducting Fault Current Limiters Are Becoming a Mature Technology," *IEEE Transactions on Applied Superconductivity*, vol. 25, no. 3, pp. 40–45, 2015.

[7] L. Quéval, F. Trillaud and B. Douine, "DC grid stabilization using a resistive superconducting fault current limiter," *International Conference on Components and Systems for DC grids (COSYS-DC 2017)*, pp. 1–11, 2017.

[8] H. J. Schettino, R. de Andrade Jr, A. Polasek, D. Kottonau, W. T. B. de Sousa, "A strategy for protection of high voltage systems using resistive superconducting fault current limiters," *Physica C: Superconductivity and its Applications*, vol. 544, pp. 40–45, 2018.

[9] J. J. Perez-Chavez, F. Trillaud, L. M. Castro, L. Queval, A. Polasek, R. de Andrade Junior, "Generic model of Three-phase (Re)BCO Resistive Superconducting Fault Current Limiters for Transient Analysis of Power Systems," *IEEE Transactions on Applied Superconductivity*, vol. 9, no. 6, p. 5601811, 2019.

[10] F. Trillaud, "Qualitative Simulation of the Thermal and Electrical Normal-Zone Transition of 2G-HTS Solenoidal Magnets: Mathematical Model and Example," *IEEE Transactions on Applied Superconductivity*, vol. 24, no. 3, p. 4701206, 2014.

[11] L. Quéval, O. Despouys, F. Trillaud, B. Douine, "Feasibility study of a superconducting power filter for HVDC grids," *2020 22nd European Conference on Power Electronics and Applications (EPE'20 ECCE Europe), Lyon, France*, pp. 1–7, 2020.

[12] Superpower Inc., "2G HTS Wire," online, http://www.superpower-inc.com/content/2g-hts-wire.

[13] D. Guillen, C. Salas, F. Trillaud, L. M. Castro, A. T. Queiroz, G. G. Sotelo, "Impact of Resistive Superconducting Fault Current Limiter and Distributed Generation on Fault Location in Distribution Networks," *Electric Power Systems Research*, vol. 186, p. 106419, 2020.

[14] S. Elschner et al., "ENSYSTROB—Design, manufacturing and test of a 3-phase resistive fault current limiter based on coated conductors for medium voltage application," *Physica C: Superconductivity and Applications*, vol. 482, no. 3, p. 98–104, 2012.

[15] National Institute of Standard, "Cryogenic technology resources," online, https://trc.nist.gov/cryogenics/.

[16] A. K. Ghosh, "*V–I* transition and *n*-value of multifilamentary LTS and HTS wires and cables," *IEEE Transactions on Applied Superconductivity*, vol. 401, no. 1-4, pp. 15–21, 2014.

[17] H. Song, and J. Schwartz, "Stability and Quench of $YBa_2Cu_3O_{7-x}$ Coated Conductor at 4.2 K, Self-Field," *Physica C: Superconductivity and Applications*, vol. 19, no. 5, pp. 3735 – 3743, 2009.

[18] J. Chen, C. Wang, J. Chen, "Investigation on the Selection of Electric Power System Architecture for Future More Electric Aircraft," *IEEE Transactions on Transportation Electrification*, vol. 4, no. 2, pp. 563–576, 2018.

[19] J. Palmer, E. Shehab, "Modelling of cryogenic cooling system design concepts for superconducting aircraft propulsion," *IET Electrical Systems in Transportation*, pp. 1–9, 2015.

[20] M. Boll, M. Corduan, S. Biser, M. Filipenko, Q. H. Pham, S. Schlachter, P. Rostek and M. Noe, "A holistic system approach for short range passenger aircraft with cryogenic propulsion system," *Superconductor Science and Technology*, vol. 33, no. 044014, p. 14pp, 2020.

[21] J. J. Breedlove, P. J. Magari, and G. W. Miller, "Cryocooler for air liquefaction onboard large aircraft," *Advances in Cryogenic Engineering: Transactions of the cryogenic conference - CEC*, vol. 53, pp. 838–845, 2008.